Title: Self-photosensitization of non-photosynthetic bacteria for self-replicating solar-to-chemical production

Authors: Kelsey K. Sakimoto[1,2], Andrew Barnabas Wong[1,2], Peidong Yang[1,2,3,4,*]

Affiliations:

[1] Department of Chemistry, University of California, Berkeley, CA 94720, USA

[2] Materials Sciences Division, Lawrence Berkeley National Laboratory, Berkeley, CA 94720, USA

[3] Department of Materials Science and Engineering, University of California, Berkeley, CA 94720, USA

[4] Kavli Energy NanoSciences Institute, Berkeley, CA 94720, USA

[*] Correspondence to: p_yang@berkeley.edu

Abstract: The future of sustainable chemical production hinges upon improving natural photosynthesis. Neither purely artificial nor purely biological approaches seem poised to fully address solar-to-chemical synthesis. This necessitates a dual/hybrid approach: combining the highly-efficient light harvesting of inorganic semiconductors with the high specificity, low-cost, and self-replication/self-repair of biocatalysts. Here, we report the self-photosensitization of a non-photosynthetic bacterium, *Moorella thermoacetica* with cadmium sulfide (CdS) nanoparticles, enabling the photosynthesis of acetic acid from CO_2. This bacteria/inorganic-semiconductor hybrid bioprecipitates CdS nanoparticles, which serve as the light harvester to sustain cellular metabolism. This cyborgian ability to self-augment biological systems through inorganic chemistry opens a new parameter space to explore the integration of biotic and abiotic components, enabling the study and the design of the next generation of advanced solar-to-chemical technologies.

One Sentence Summary: The non-photosynthetic CO_2 reducing bacterium *Moorella thermoacetica* was self-photosensitized by the bioprecipitation of cadmium sulfide nanoparticles, enabling the photosynthetic production of acetic acid from CO_2.

Main Text: The necessity of improving the natural mechanisms of solar energy capture for sustainable chemical production (*1*) has motivated the development of photoelectrochemical devices based on inorganic, solid-state materials (*2*). While solid-state semiconductor light absorbers often exceed biological light harvesting in efficiency (*3*), transduction of photoexcited electrons into chemical bonds (particularly towards multi-carbon compounds from CO_2) remains challenging for abiotic catalysts (*4*, *5*). Such catalysts struggle to compete with the high specificity, low-cost material requirements, and self-replicating/self-repairing properties of biological CO_2 fixation (*6*). Thus, a likely solution must combine the best of both worlds: the light harvesting capabilities of semiconductors with the catalytic power of biology.

Several inorganic-biological hybrid systems have been devised: semiconductor nanoparticles with hydrogenases to produce biohydrogen (*7*), long wavelength absorbing nanomaterials to improve the efficiency of plants (*8*), or whole-cells with photoelectrodes for CO_2 fixation (*9*, *10*). Whole-cell microorganisms are favored to facilitate the multi-step process of CO_2 fixation and can self-replicate/self-repair (*11*). Furthermore, bacteria termed electrotrophs undergo direct electron transfer from an electrode (*12*). However, traditional chemical synthesis of the semiconductor component requires high-purity reagents, high temperatures, and complex microfabrication techniques. Additionally, the integration of foreign materials with biotic systems is non-trivial (*13*). Many reports have shown that some microorganisms bioprecipitate nanoparticles (*14*), producing an inherently biocompatible nanomaterial under mild conditions.

While photosynthetic organisms can bioprecipitate semiconductor nanoparticles, their metabolic pathways are arguably less desirable than their non-photosynthetic counterparts. Though gene modification of phototrophs has progressed (*15*), non-photosynthetic bacteria remain the workhorse of synthetic biology, offering a facile route to tailoring the product

diversity from CO_2 reduction (*16*). Additionally, thermodynamic comparisons reveal significant energetic advantages to photosensitizing non-photosynthetic CO_2 reduction (*17*). Of particular interest is the Wood-Ljungdahl pathway through which CO_2 is reduced to acetyl coenzyme A (acetyl-CoA), a common biosynthetic intermediate, and eventually acetic acid, both of which can be further upgraded to high-value products by wild-type and genetically engineered organisms (*10*, *18*). This pathway is also used by CO_2 fixing electrotrophs, enabling the use of semiconductor photoelectrons in this energetically efficient biosynthetic route.

As a proof-of-concept, we show that *Moorella thermoacetica* can utilize self-bioprecipitated CdS to photosynthesize acetic acid from light and CO_2. With an appropriate band structure, CdS is a well-studied semiconductor suitable for photosynthesis (*19*). As an acetogen and an electrotroph, *M. thermoacetica* serves as an ideal model organism to explore the capabilities of this hybrid system (*20*). The photosynthesis of acetic acid by *M. thermoacetica*/CdS is a two-step, one-pot synthesis (Fig. 1): First, the precipitation of CdS by *M. thermoacetica* triggered by the addition of Cd^{2+} and cysteine (Cys) as the sulfur source (*21*):

$$Cd^{2+} + Cys \xrightarrow{M.\,thermoacetica} CdS + NH_3 + \text{pyruvic acid} + 2\,H^+ \quad (1)$$

M. thermoacetica utilizes photogenerated electrons from illuminated CdS nanoparticles to carry out photosynthesis (Fig. 1B). Absorption of a photon, $h\nu$, by CdS produces an electron-hole pair, e^- and h^+:

$$h\nu \xrightarrow{CdS} e^- + h^+ \quad (2)$$

The electron generates a reducing equivalent, [H], (see supplementary online text and Fig. S1 for elaboration of this process):

$$2\,H^+ + 2\,e^- \xrightarrow{M.\,thermoacetica\,/\,CdS} 2\,[H] \quad (3)$$

which is then passed on to the Wood-Ljungdahl pathway to synthesize acetic acid from CO_2:

$$2\ CO_2 + 8\ [H] \xrightarrow{M.\ thermoacetica\ /\ CdS} CH_3COOH + 2\ H_2O \quad (4)$$

Cysteine quenches the h^+ leading to the oxidized disulfide form, cystine (CySS):

$$2\ Cys + 2\ h^+ \xrightarrow{M.\ thermoacetica\ /\ CdS} CySS + 2\ H^+ \quad (5)$$

Combining and balancing Eq. 2 to 5 yields the overall photosynthetic reaction:

$$2\ CO_2 + 8\ Cys + 8\ h\nu \xrightarrow{M.\ thermoacetica\ /\ CdS} CH_3COOH + 2\ H_2O + 4\ CySS \quad (6)$$

M. thermoacetica/CdS, a hybrid inorganic-biological organism, demonstrates photosynthetic behavior comparable to natural photosynthesis, employing both the superior light harvesting of inorganic semiconductors, and the self-replicating/self-repairing, high performance CO_2 fixation of biological systems.

Bioprecipitation of CdS by *M. thermoacetica* (ATCC 39073) was initiated by addition of $Cd(NO_3)_2$ to an early exponential growth culture of glucose-grown cells supplemented with Cys (Fig. S2) (*22*). Initially, a white precipitate formed, ascribed to the nucleation of small, quantum confined CdS nanoparticles (Fig. S3C) that upon further incubation formed an opaque yellow suspension (Fig. S2D). Scanning electron microscopy (SEM) revealed <50 nm particles decorating the cell surface (Fig. 2A and B). Incubation for extended periods of time (>3 days) formed larger particles (~100 nm, Fig. 2C). Scanning transmission electron microscopy (STEM) and energy dispersive x-ray spectroscopy (EDS) mapping revealed that the ~50 nm particles were clusters of smaller nanoparticles (<10 nm, Fig. 3A and B) composed of cadmium and sulfur (Fig. 3, C to E), with occasional minor components of phosphorous and oxygen, possibly $Cd_3(PO_4)_2$ (Fig. S4, D, E and H).

Absorption spectra and Tauc plots yielded a measured direct band gap of 2.51±0.05 eV (Fig. S5A). The slightly larger measured band gap compared to bulk CdS (2.42 eV) suggests

quantum confinement expected of sub-10 nm particles (*19*). Powder x-ray diffraction (XRD) displayed broad peaks consistent with small particles of the wurtzite phase (Fig. S5B).

Following bioprecipitation, *M. thermoacetica*/CdS was resuspended in a defined medium containing no organic carbon sources aside from trace amounts of vitamins and Cys. To confirm photosynthesis, a series of deletional controls were carried out in which *M. thermoacetica*, CdS, and light were systematically removed (Fig. 4, A and B).

In the absence of light (405±5 nm), acetic acid concentrations measured by quantitative proton nuclear magnetic resonance (^{1}H-qNMR) spectroscopy decreased (from ~2 mM accumulated under initial H_2:CO_2 acclimation) potentially due to a dark catabolic process. The viability determined by colony forming units (CFU) assays slowly declined to ~25% after 4 days (initially $5.9\pm0.4\times10^4$ CFU mL^{-1} and $1.7\pm0.4\times10^9$ cells mL^{-1}) indicating that *M. thermoacetica*/CdS requires light to maintain viability. The viability of bare *M. thermoacetica* without CdS dropped to 0% within the first day under light, consistent with previous observations of semiconducting/insulating precipitates having a photoprotective role towards bacteria (*23*). Only *M. thermoacetica*/CdS hybrids with light produced acetic acid. The ^{1}H-qNMR spectrum revealed acetic acid to be the only CO_2 reduction product, confirming the high selectivity expected of biological catalysts (Fig. S6). After the first 1.5 days, the rate of production began to plateau because of the limiting amounts of the sacrificial reductant, Cys.

A maximum yield of ~90% acetic acid (based on the initial Cys concentration) was calculated, which is consistent with previous observations that ~10% of reduced CO_2 under the Wood-Ljungdahl pathway is directed towards cell biomass (*24*). Under photosynthesis, both the viability and cell counts of *M. thermoacetica*/CdS nearly double after the first day (Fig S7), on par with the doubling time of autotrophic growth (~25 hrs). While the growth is not vigorous and

perhaps limited by the total amount of CdS and other nutrients, these results suggest the possibility of a completely self-reproducing hybrid organism sustained purely through solar energy. After the third and fourth day, viability decreases, coincidental with the depletion of Cys, leading to oxidative photodamage (Fig. S8).

Under increasing blue light (435-485 nm) flux, the rate of acetic acid production increased (Fig. 4C). At 5×10^{13} photons cm^{-2} s^{-1}, a quantum yield of 52±17% was observed. The rate of photosynthesis increased up until 160×10^{13} photons cm^{-2} s^{-1} when the rate dramatically decreased and the quantum yield dropped to 4±1%, possibly due to photooxidative degradation under high light intensities (*25*). Under high light flux, large holes formed in the cell surface, and in some cases, resulted in the complete destruction of the cell membrane (Fig. S8). The high quantum yield of *M. thermoacetica*/CdS is notable given previous analogous systems often report quantum efficiencies of ~20% (*7*). This result is rationalized by the low light flux of these measurements, which reduces losses from recombination (*26*). To explore this idea, higher concentrations of *M. thermoacetica*/CdS were measured (Fig. 4C). With 4× the normal *M. thermoacetica*/CdS loading, a quantum yield of 85±12% was measured. Under higher concentrations, the average flux per bacteria is decreased, correlating with increased quantum yield.

To further characterize their photosynthetic behavior, *M. thermoacetica*/CdS was illuminated under low-intensity simulated sunlight (AM 1.5G spectrum, 2 W m^{-2}) with a 12 hr light/dark cycle to mimic day/night cycles (Fig. 4D). Unexpectedly, acetic acid concentrations not only increased under illumination, but continued to increase through the dark at the same rate through several light/dark cycles. A potential explanation lies in the build up of biosynthetic intermediates during the light cycle, which are then utilized during the dark cycle. These may

include a number of reductive species (NADH, NADPH, ferredoxin), or intermediates in the Wood-Ljungdahl pathway such as acetyl-CoA (*27*). A proton gradient may also be storing energy for ATP synthesis in the dark. Further experiments varying the duration of the light cycle (Fig. 4E) revealed a proportionality between the length of illumination, τ, and the dark acetic acid yield. While the initial rate during and just after illumination appears to be relatively constant, consistent with a zeroth order catalytic reaction, the yield begins to plateau after 2τ, exhibiting a linearity between illumination time and acetic acid yield (Fig. 4E, inset). However, at 5τ, the 24 hr illuminated sample breaks this trend. These observations suggest that up through 12 hours of illumination, some intermediate accumulates, giving proportional dark acetic acid yield. Beyond this, the intermediate may saturate, giving no further acetic acid yield with longer illumination. A peak quantum yield of 2.44±0.62% of total incident low-intensity simulated sunlight was measured (Fig. 4D). These quantum yields are order-of-magnitude comparable with the year-long averages determined for plants and algae which range from ~0.2-1.6% (*1*).

Biological routes to solid-state materials have often struggled to compete with high-quality, traditionally synthesized materials. This work demonstrates not only that biomaterials can be of sufficient quality to carry out useful photochemistry, but in some ways may be more advantageous in biological applications. Most traditional nanoparticle syntheses require organic capping ligands to control particle shape. These ligands present a barrier to charge transfer between semiconductor and catalyst, often relying upon electron tunneling (*13*). The ligand-free approach taken here may help in establishing a favorable interface between bacteria and semiconductor, resulting in the high efficiencies. Additionally, metal chalcogenides (such as CdS) have found limited application due to oxidative photodegradation. The ability of bacteria to precipitate metal chalcogenides from the products of photodissolution, (Cd^{2+} and oxidized sulfur

complex ions) suggests a potential regenerative pathway to circumvent the debilitating photoinstability through a bioprecipitative self-regeneration.

Surprisingly, *M. thermoacetica*/CdS displays behavior that may help it to exceed the utility of natural photosynthesis. First, quantum yield increased with higher *M. thermoacetica*/CdS concentrations. The ability to tune the effective light flux per bacteria by simply changing the concentration of the suspension is a large advantage over similar light management practices in natural photosynthesis achieved through genetic engineering of chloroplast expression (*28*). Secondly, the catabolic energy loss observed in natural photosynthesis during dark cycles was absent in *M. thermoacetica*/CdS, which perhaps may be an innate feature of the Wood-Ljungdahl pathway, in which acetic acid is a waste product of normal respiration. Additionally, many plants and algae tend to store a large portion of their photosynthetic products as biomass, which requires significant processing to produce useful chemicals. In contrast, *M. thermoacetica*/CdS, directs ~90% of photosynthetic products towards acetic acid, reducing the cost of diversifying to other chemical products.

To improve this system, greater utility could be gained by substituting Cys oxidation with a more beneficial oxidation reaction, such as oxygen evolution, wastewater oxidation for water purification, or oxidative biomass conversion (*29*, *30*). Expanding the material library available through bioprecipitation will increase light absorption and raise the upper limit on bacteria/semiconductor photosynthetic efficiency. The availability of genetic engineering tools for *M. thermoacetica* (*31*), as well as introduction of electrotrophic and bioprecipitation behavior in model bacteria such as *Escherichia coli* (*32*, *33*), suggests a potential role for synthetic biology in rationally designing such hybrid organisms.

Beyond the development of advanced solar-to-chemical synthesis platforms, this hybrid organism also holds potential as a tool to study biological systems. The native integration of semiconductor nanoparticles with bacterial metabolic processes provides a unique optical tag for the study of microbial behavior, such as semiconductor-bacteria electron transfer (*34*, *35*), by providing a sensitive, non-invasive, non-chemical probe. The ability of single-celled organisms to augment their functionality with foreign materials, a cyborgian trait certainly observed in humans and other complex organisms opens up a new parameter space to design advanced biological systems, as well as uncover the surprising ways in which nature conducts chemistry.

Supplementary Materials:

www.sciencemag.org

Materials and Methods

Supplementary Text

Figures S1-S9

References and Notes:

1. A. W. D. Larkum, Limitations and prospects of natural photosynthesis for bioenergy production. *Curr. Opin. Biotechnol.* **21**, 271–276 (2010).

2. D. Gust, T. A. Moore, A. L. Moore, Solar Fuels via Artificial Photosynthesis. *Acc. Chem. Res.* **42**, 1890–1898 (2009).

3. R. E. Blankenship *et al.*, Comparing Photosynthetic and Photovoltaic Efficiencies and Recognizing the Potential for Improvement. *Science.* **332**, 805–809 (2011).

4. T. J. Meyer, Chemical Approaches to Artificial Photosynthesis. *Acc. Chem. Res.* **22**, 163–170 (1989).

5. A. M. Appel *et al.*, Frontiers, Opportunities, and Challenges in Biochemical and Chemical Catalysis of CO_2 Fixation. *Chem. Rev.* **113**, 6621–6658 (2013).

6. A. S. Hawkins, P. M. McTernan, H. Lian, R. M. Kelly, M. W. W. Adams, Biological conversion of carbon dioxide and hydrogen into liquid fuels and industrial chemicals. *Curr. Opin. Biotechnol.* **24**, 376–84 (2013).

7. K. A. Brown, M. B. Wilker, M. Boehm, G. Dukovic, P. W. King, Characterization of photochemical processes for H_2 production by CdS nanorod-[FeFe] hydrogenase complexes. *J. Am. Chem. Soc.* **134**, 5627–5636 (2012).

8. J. P. Giraldo *et al.*, Plant nanobionics approach to augment photosynthesis and biochemical sensing. *Nat. Mater.* **13**, 400–408 (2014).

9. J. P. Torella *et al.*, Efficient solar-to-fuels production from a hybrid microbial–water-splitting catalyst system. *Proc. Natl. Acad. Sci.* **112**, 2337–2342 (2015).

10. C. Liu *et al.*, Nanowire–Bacteria Hybrids for Unassisted Solar Carbon Dioxide Fixation to Value-Added Chemicals. *Nano Lett.* **15**, 3634–3639 (2015).

11. L. Lapinsonnière, M. Picot, F. Barrière, Enzymatic versus Microbial Bio-Catalyzed Electrodes in Bio-Electrochemical Systems. *ChemSusChem*. **5**, 995–1005 (2012).

12. K. P. Nevin *et al.*, Electrosynthesis of Organic Compounds from Carbon Dioxide Is Catalyzed by a Diversity of Acetogenic Microorganisms. *Appl. Environ. Microbiol.* **77**, 2882–2886 (2011).

13. P. W. King, Designing interfaces of hydrogenase-nanomaterial hybrids for efficient solar conversion. *Biochim. Biophys. Acta*. **1827**, 949–957 (2013).

14. W. J. Crookes-Goodson, J. M. Slocik, R. R. Naik, Bio-directed synthesis and assembly of nanomaterials. *Chem. Soc. Rev.* **37**, 2403–2412 (2008).

15. D. C. Ducat, P. A. Silver, Improving carbon fixation pathways. *Curr. Opin. Chem. Biol.* **16**, 337–44 (2012).

16. L. S. Gronenberg, R. J. Marcheschi, J. C. Liao, Next generation biofuel engineering in prokaryotes. *Curr. Opin. Chem. Biol.* **17**, 462–471 (2013).

17. A. G. Fast, E. T. Papoutsakis, Stoichiometric and energetic analyses of non-photosynthetic CO2-fixation pathways to support synthetic biology strategies for production of fuels and chemicals. *Curr. Opin. Chem. Eng.* **1**, 380–395 (2012).

18. M. C. A. A. Van Eerten-Jansen *et al.*, Bioelectrochemical Production of Caproate and Caprylate from Acetate by Mixed Cultures. *ACS Sustain. Chem. Eng.* **1**, 513–518 (2013).

19. R. Vogel, P. . Hoyer, H. Weller, Quantum-sized PbS, CdS, Ag_2S, Sb_2S_3, and Bi_2S_3 Particles as Sensitizers for Various Nanoporous Wide-Bandgap Semiconductors. *J. Phys. Chem.* **98**, 3183–3188 (1994).

20. H. L. Drake, S. L. Daniel, Physiology of the thermophilic acetogen Moorella thermoacetica. *Res. Microbiol.* **155**, 869–883 (2004).

21. D. P. Cunningham, L. L. Lundie, Precipitation of cadmium by Clostridium thermoaceticum. *Appl. Environ. Microbiol.* **59**, 7–14 (1993).

22. Materials and methods are available as supplementary materials on *Science* Online.

23. J. D. Holmes *et al.*, Bacterial Photoprotection Through Extracellular Cadmium Sulfide Crystallites. *Photochem. Photobiol.* **62**, 1022–1026 (1995).

24. S. L. Daniel, T. Hsu, S. I. Dean, H. L. Drake, L. Ljungdahl, Characterization of the H_2- and CO-Dependent Chemolithotrophic Potentials of the Acetogens Clostridium thermoaceticum and Acetogenium kivuit. *J. Bacteriol.* **172**, 4464–4471 (1990).

25. E. Dumas *et al.*, Interfacial Charge Transfer between CdTe Quantum Dots and Gram Negative Vs Gram Positive Bacteria. *Environ. Sci. Technol.* **44**, 1464–1470 (2010).

26. B. Liu, X. Zhao, C. Terashima, A. Fujishima, K. Nakata, Thermodynamic and kinetic analysis of heterogeneous photocatalysis for semiconductor systems. *Phys. Chem. Chem. Phys*. **16**, 8751–8760 (2014).

27. K. Schuchmann, V. Müller, Autotrophy at the thermodynamic limit of life: a model for energy conservation in acetogenic bacteria. *Nat. Rev. Microbiol.* **12**, 809–821 (2014).

28. B. Hankamer *et al.*, Photosynthetic biomass and H_2 production by green algae: From bioengineering to bioreactor scale-up. *Physiol. Plant.* **131**, 10–21 (2007).

29. H. G. Cha, K.-S. Choi, Combined biomass valorization and hydrogen production in a photoelectrochemical cell. *Nat. Chem.* **7**, 328–333 (2015).

30. B. E. Logan, K. Rabaey, Conversion of Wastes into Bioelectricity and Chemicals by using Microbial Electrochemical Technologies. *Science.* **337**, 686–690 (2012).

31. A. Kita *et al.*, Development of genetic transformation and heterologous expression system in carboxydotrophic thermophilic acetogen Moorella thermoacetica. *J. Biosci. Bioeng.* **115**, 347–352 (2013).

32. H. M. Jensen *et al.*, Engineering of a synthetic electron conduit in living cells. *Proc. Natl. Acad. Sci.* **107**, 19213–19218 (2010).

33. C. L. Wang, A. M. Lum, S. C. Ozuna, D. S. Clark, J. D. Keasling, Aerobic sulfide production and cadmium precipitation by Escherichia coli expressing the Treponema denticola cysteine desulfhydrase gene. *Appl. Microbiol. Biotechnol.* **56**, 425–430 (2001).

34. M. Rosenbaum, F. Aulenta, M. Villano, L. T. Angenent, Cathodes as electron donors for microbial metabolism: Which extracellular electron transfer mechanisms are involved? *Bioresour. Technol.* **102**, 324–33 (2011).

35. J. S. Deutzmann, M. Sahin, A. M. Spormann, Extracellular Enzymes Facilitate Electron Uptake in Biocorrosion and Bioelectrosynthesis. *MBio*. **6**, 1–8 (2015).

Acknowledgments: This work is supported by National Science Foundation **(**DMR-1507914). The authors thank Joseph J. Gallagher and Michelle C.Y. Chang for the original inoculum of *M. thermoacetica* ATCC 39073. K.K.S acknowledges the National Science Foundation Graduate Research Fellowship Program under Grant No. DGE 1106400. The authors thank the National Center for Electron Microscopy. Work at the Molecular Foundry was supported by the Office of Science, Office of Basic Energy Sciences, of the U.S. Department of Energy under Contract No. DE-AC02-05CH11231. All data presented in the paper is available in the body of the paper or in the Supplementary Materials.

Fig. 1. *M. thermoacetica*/CdS Reaction Schematics. (**A**) Depiction of the growth of *M thermoacetica*/CdS proceeding through 1) growth of the cells and bioprecipitation/loading of CdS nanoparticles followed by 2) photosynthesis of CO_2 to acetic acid. (**B**) Pathway diagram for *M. thermoacetica*/CdS (Eq. 1-6). Two possible routes to generate reducing equivalents, [H], exist: generation outside the cell (dashed line), or generation by direct electron transport to the cell (solid line). Hypothesized electron transfer pathways are presented in Fig. S1.

Fig. 2. SEM of *M. thermoacetica*/CdS Hybrids. (**A** and **B**) Bioprecipitated CdS nanoparticles on *M. thermoacetica*. (**C**) Larger nanoparticles observed after extended incubation. (**D**) A smooth, undecorated cell shown for reference. All scale bars are 1 μm.

Fig. 3. STEM of *M. thermoacetica*/CdS Hybrids. (**A**) STEM of a single cell showing clusters decorated across the entire cell. (**B**) High Angle Annular Dark Field (HAADF) image (higher magnification of box in **A)**. (**C**) EDS mapping showing clusters mainly composed of (**D**) cadmium and (**E**) sulfur. Further elemental mapping is provided in Fig. S4. Scale bars are (**A**) 500 nm, (**B**) 100 nm, (**C** to **D**) 50 nm.

Fig. 4. Photosynthesis Behavior of *M. thermoacetica*/CdS Hybrids. (**A**) Photosynthetic production of acetic acid for *M. thermoacetica*/CdS and deletional controls. Key applies to (**A** and **B**) only. (**B**) CFU viability assays for *M. thermoacetica*/CdS and deletional controls. (**C**) The rate of acetic acid production and quantum yield for increasing illumination intensities and increased *M. thermoacetica*/CdS concentrations. (**D**) Photosynthetic acetic acid production under low intensity simulated sunlight with light/dark cycles. (**E**) Acetic acid production in dark for varying illumination times. Inset shows the relation between illumination time, τ, and acetic acid yield at increasing multiples of τ in dark. All values and error bars represent the mean and error propagated standard deviation of triplicate experiments.

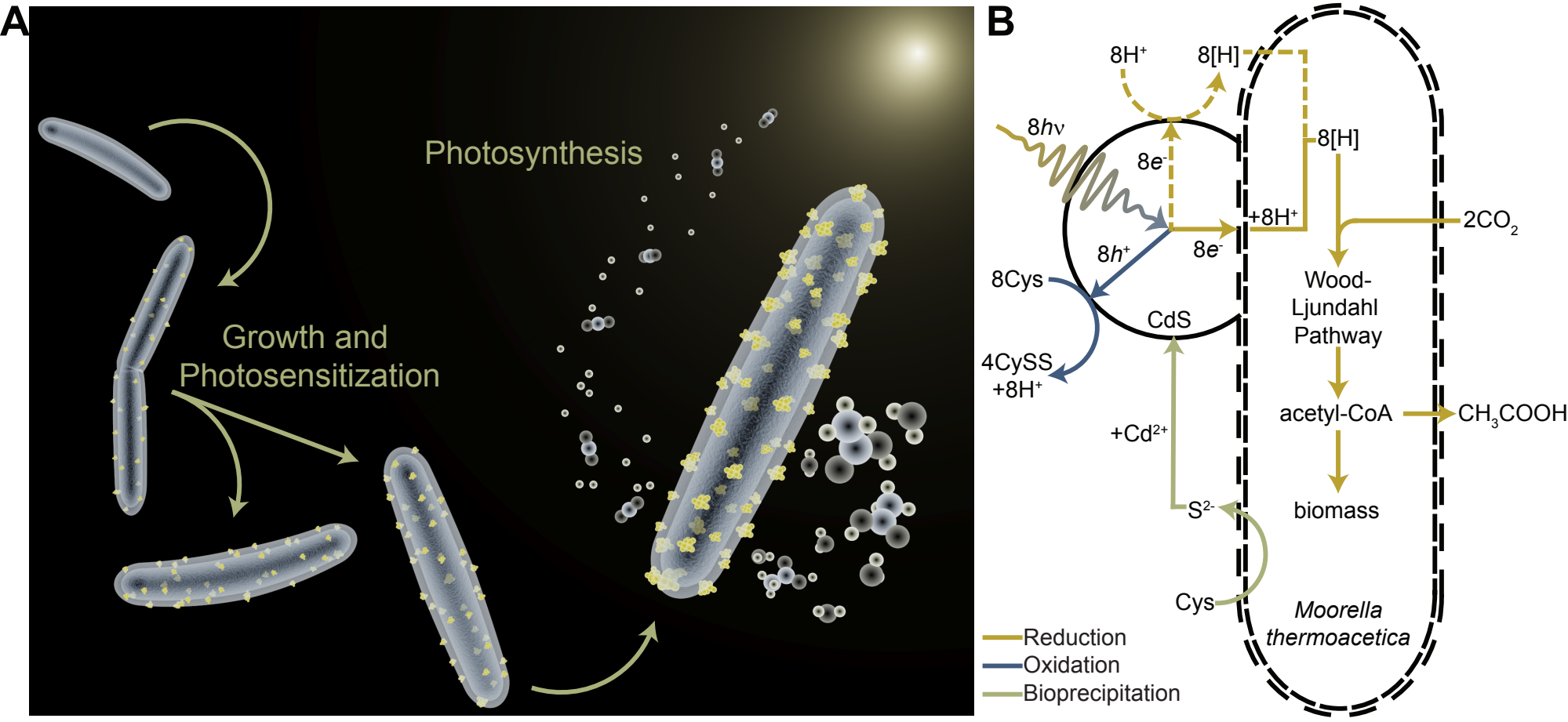
A
Photosynthesis
Growth and
Photosensitization
B
8H+
8[H]
8hν
8e-
8[H]
+8H+
2CO2
8h+
8e-
8Cys
Wood-
Ljundahl
Pathway
CdS
4CySS
+8H+
+Cd2+
acetyl-CoA
CH3COOH
biomass
S2-
Cys
Moorella
thermoacetica
Reduction
Oxidation
Bioprecipitation

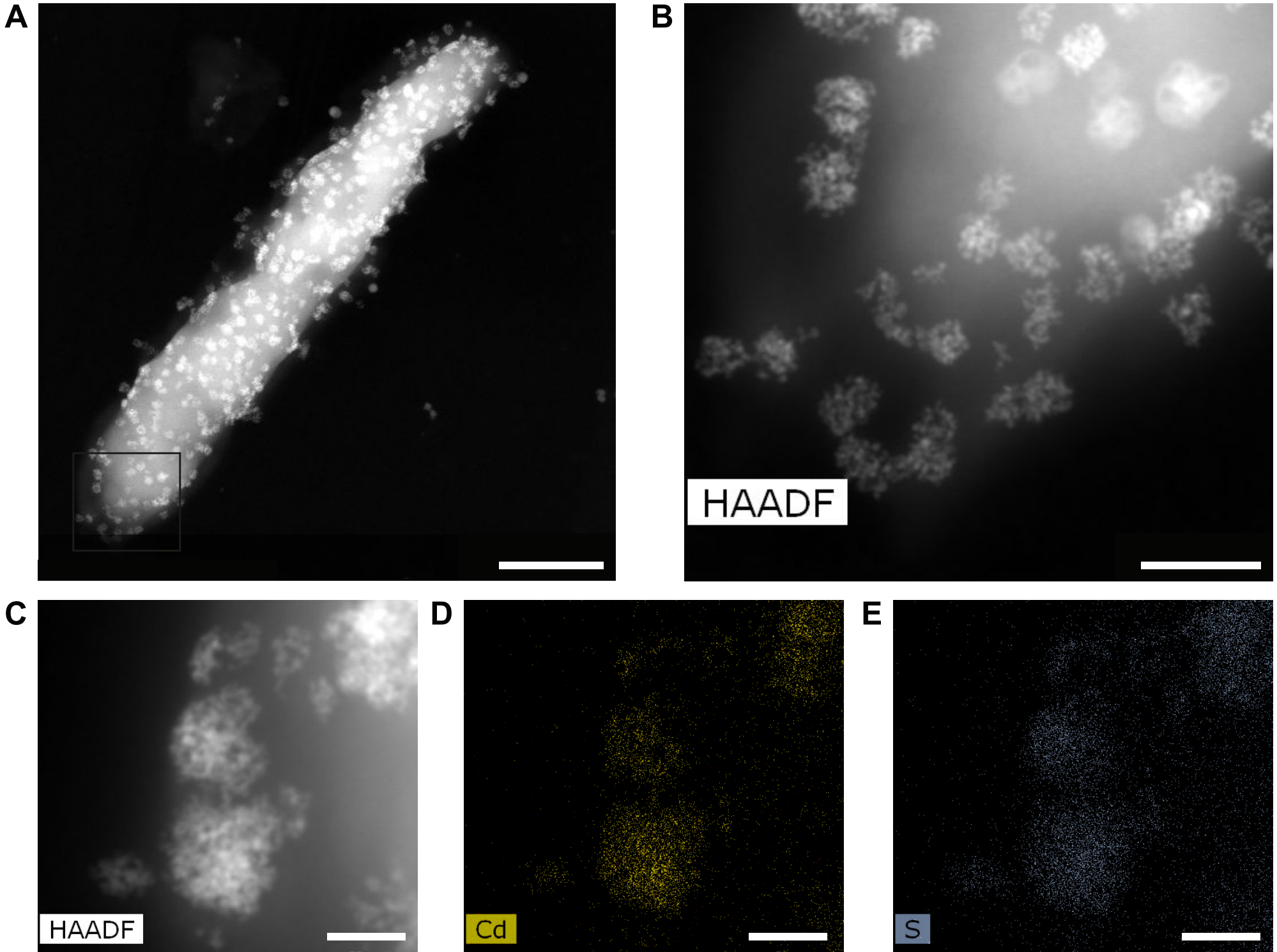
A
B
HAADF
C
HAADF
D
Cd
E
S

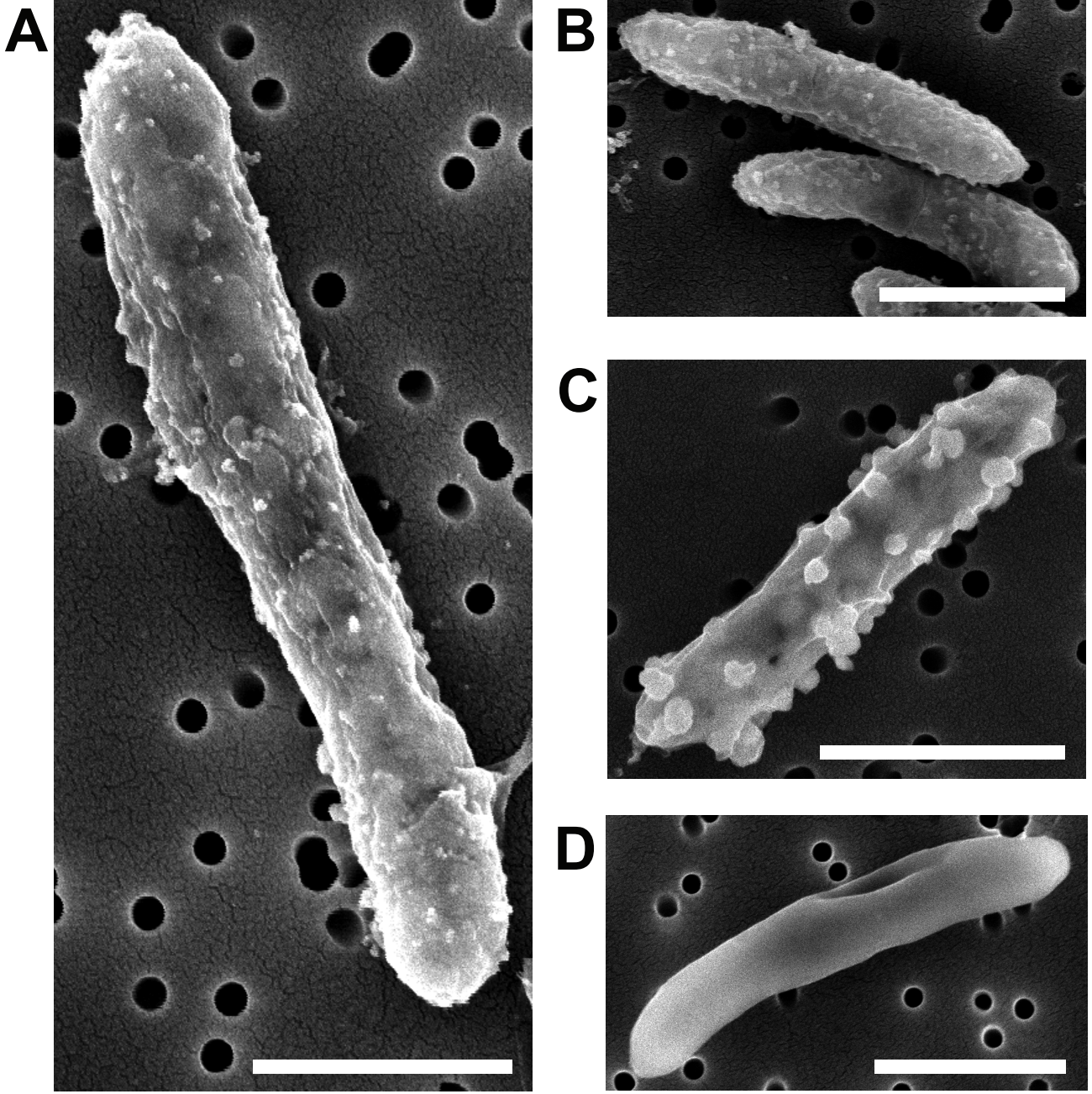
A
B
C
D

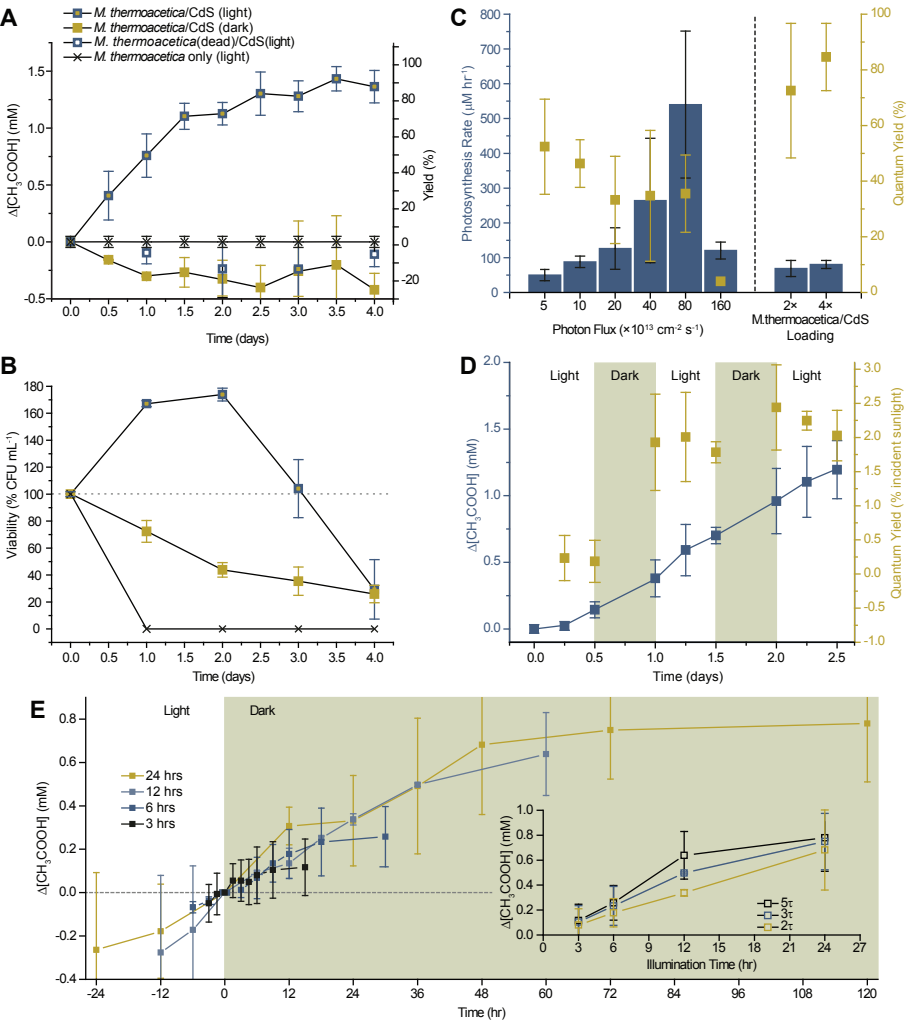
A
M. thermoacetica/CdS (light)
M. thermoacetica/CdS (dark)
M. thermoacetica(dead)/CdS(light)
M. thermoacetica only (light)
Δ[CH3COOH] (mM)
Yield (%)
Time (days)
B
Viability (% CFU mL-1)
Time (days)
C
Photosynthesis Rate (μM hr-1)
Quantum Yield (%)
Photon Flux (×10^13 cm-2 s-1)
M.thermoacetica/CdS Loading
2×
4×
D
Light
Dark
Light
Dark
Light
Δ[CH3COOH] (mM)
Quantum Yield (% incident sunlight)
Time (days)
E
Light
Dark
24 hrs
12 hrs
6 hrs
3 hrs
Δ[CH3COOH] (mM)
Time (hr)
Illumination Time (hr)
5τ
3τ
2τ